



## UPPER MANTLE ATTENUATION STRUCTURE BENEATH THE EASTERN HOKKAIDO, JAPAN AND ITS EFFECTS ON STRONG GROUND MOTIONS

Takahiro MAEDA<sup>1</sup> and Tsutomu SASATANI<sup>2</sup>

### SUMMARY

It is especially important for predicting strong ground motion from large intra-slab earthquakes to estimate upper mantle attenuation ( $Q$ ) structure beneath island-arc regions. We investigate effects of the upper mantle  $Q$  structure on strong ground motions based on numerous data observed at dense strong motion stations in the eastern part of Hokkaido, Japan. First we investigate strong motion records and their  $S$ -wave spectra from intermediate-depth earthquakes. The  $S$ -wave spectra at stations on the fore-arc side of the volcanic front (VF) are extremely different from those on the back-arc side; the  $S$ -wave spectra at the back-arc side stations severely lack in high-frequency contents. Next we estimate the  $Q_s$  ( $Q$ -value for  $S$ -wave) structure beneath the eastern Hokkaido. The study zone is tentatively divided into three zones bounded by a coastline and the VF; the three zones mainly correspond to a back-arc side mantle wedge (BAMW), a fore-arc side mantle wedge (FAMW) and a shallow descending plate. We especially use strong motion data obtained by ocean bottom seismometers for plate  $Q_s$  estimate. Two different methods, the spectral inversion and the coda-normalization method, are applied to  $Q_s$  estimate for the FAMW and plate. The  $Q_s$ -values for these two zones are nearly the same and show strong frequency-dependence. The  $Q_s$ -values obtained from two methods are nearly the same. We also estimate  $Q_s$ -values for the BAMW by using the  $S$ -wave spectra observed at stations on the back-arc side of the VF and the source spectra obtained from the spectral inversion. Although the data set for the BAMW is incomplete due to few records and low signal-to-noise ratios of  $S$ -wave spectra, we suggest that the  $Q_s$ -values for the BAMW have considerably weak frequency-dependence. Finally we examine the attenuation structure of the plate, because the estimated  $Q_s$  value in this study seems to be small compared with past studies. We assume two-layer  $Q_s$  structure for the plate and obtain high  $Q_s$  value in the lower layer. We conclude that the anomalous upper mantle attenuation structure beneath the eastern Hokkaido reflects the difference in the frequency-dependence of  $Q_s$ -value at high-frequencies ( $>1\text{Hz}$ ). The laterally heterogeneous  $Q_s$  structure obtained in this study is useful for predicting strong ground motion from large intra-slab earthquakes such as the 1993 Kushiro-oki earthquake.

### INTRODUCTION

---

<sup>1</sup> Post Doc. Res. Fellow, Hokkaido Univ. Sapporo, Japan, Email: tmaeda@ares.sci.hokudai.ac.jp

<sup>2</sup> Asso. Prof., Hokkaido Univ. Sapporo, Japan, Email: sasatani@ares.sci.hokudai.ac.jp

It is well known that there exists the anomalous upper mantle structure beneath island-arc regions; the high Q and high velocity zone, that is the descending plate or slab, sinks into the low Q and low velocity upper mantle. Estimation of Q values, especially Q values for S-waves ( $Q_s$ ), of the plate and the surrounding zone is indispensable for the quantitative prediction of strong ground motions from the viewpoint of disaster mitigation for large plate-boundary and intra-slab earthquakes. Recently the 3-D attenuation structure of the Japanese island-arc has been estimated by inversion of seismic data (e.g. Umino and Hasegawa[1]; Nakamura and Uetake[2]; Tsumura et al.[3]) and these studies have concluded that the high Q regions generally correspond to the plate or the slab. These studies, however, used data recorded at land stations. In this case, the majority of the seismic rays pass through a zone outside of the plate and it means that the resolving power for estimation of the plate's Q values for these data is poor.

In this study, we estimate the  $Q_s$  structure in the southernmost Kurile-Hokkaido arc. To accomplish this purpose, we apply two methods of  $Q_s$  estimation to seismic data recorded at ocean bottom stations as well as at land stations. The seismic data obtained at the ocean bottom stations are used in the plate's  $Q_s$  estimation. For these data, the seismic ray passes mainly through the plate and its enable us to more directly estimate plate's  $Q_s$  values compared with past studies.

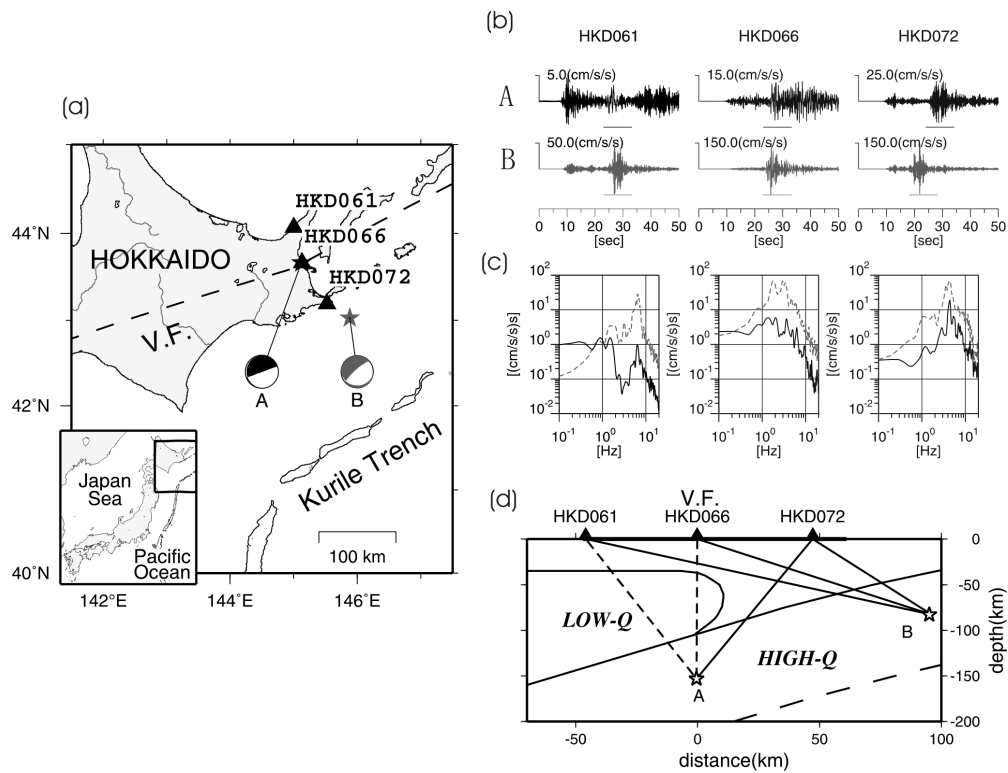


**Figure 1.** (a) Location map showing the stations (triangles) and events (stars). A dashed line denotes the volcanic front. Map inset show the study area. (b) Accelerograms (NS component) recorded at three stations from two events. (c) S-wave acceleration Fourier spectra calculated for the portion shown by the underline in (b). Black lines show the spectra from event A, and gray dashed lines show those from event B. (d) Schematic  $Q_s$  structure beneath the study zone (a vertical section perpendicular to the Kurile arc). The high-Q zone is corresponding to the Pacific plate or slab.

## QUALITATIVE EVALUATION OF QS STRUCTURE

In this section, we qualitatively investigate an attenuation structure beneath the eastern Hokkaido by comparing strong-motion records from intermediate-depth events. Fig. 1(a) shows the stations and earthquakes used. These are the K-NET strong-motion stations deployed by National Research Institute for Earth Science and Disaster Prevention (NIED) where strong motion accelerometer, K-NET95, have been equipped on the ground surface. HKD061 is located on the back-arc side of the volcanic front (VF), HKD066, just on the VF, and HKD072, on the fore-arc side of the VF. An intermediate-depth event A (1997/11/15, Mj=6.1) has a focal depth of about 150 km, while the other event B (2001/04/27, Mj=5.9) has a focal depth of about 80 km. The envelopes of accelerograms at three stations from event B are well alike mutually as shown in Fig. 1(b). Those from event A, however, show different features among stations: large later phases are found in HKD061 and HKD066 seismograms, that are consider to be scattered waves. Fig. 1(c) shows the S-wave spectra. The difference of the amplitude level between two events at high frequencies more than about 1Hz become large at the northern stations. We can mainly attribute this difference to the path effect that results from the anomalous upper mantle structure. The seismic rays from the event A to the northern stations pass through the low Q zone, but the rays from the events A and B to the southern stations pass through the high Q zone as shown in Fig. 1(d).

### ANALYSIS

#### Method

The amplitude spectrum of direct S-wave ( $O_{ij}(f)$ ) in a homogeneous structure can be expressed as

$$O_{ij}(f) = S_i(f)G_j(f) \frac{1}{R_{ij}} \exp\left(\frac{-\pi f t_{ij}}{Q_S(f)}\right), \quad (1)$$

where  $S_i(f)$  and  $G_j(f)$  represent the source spectrum of  $i$ -th event and the site amplification factor at  $j$ -th station, respectively. Although these factors are dependent on source-to-station direction, we can eliminate those dependencies by using various direction data.  $Q_S(f)$  represents the path-averaged quality factor for S-wave,  $t_{ij}$  and  $R_{ij}$  are the S-wave travel time and the hypocentral distance between  $i$ -th event and  $j$ -th station, respectively.  $S_i(f)$  and  $G_j(f)$  as well as  $Q_S(f)$  affect the characteristics of the observed seismograms as shown in eq.(1), thus it is impossible to evaluate  $Q_S(f)$  from seismograms directly. We applied two techniques of Qs estimation, the spectral inversion method (SI; Iwata and Irikura[4]) and the coda-normalization method (CN; Aki[5]). The SI method estimates not only  $Q_S(f)$  but  $S_i(f)$  and  $G_j(f)$  from multi-event and multi-station spectra. On the other hand, the CN method needs single-station spectra for Qs estimation. The good agreement of the result from two techniques guarantees the reliability of the Qs estimates.

#### (a) Spectral inversion method

Logarithm of eq. (1) is expressed as follows,

$$\log(O'_{ij}(f)) = \log(S'_i(f)) + \log(G_j(f)) - \log(e) \frac{\pi f t_{ij}}{Q_S(f)} \quad (2)$$

where  $O'_{ij} = (R_{ij}/R_{ref})O_{ij}$ ,  $S'_i = S_i/R_{ref}$ .  $R_{ref}$  is the arbitrary normalized distance and  $e$  is the Napier's number. The unknown parameters,  $S_i(f)$ ,  $G_j(f)$  and  $Q_S(f)$ , are determined by minimizing the residual between eq. (2) and observed spectra in least square sense. We solve this least square problem with two linear inequality constraints ( $G_j(f) \geq 2$  and  $Q_S^{-1}(f) \geq 1000^{-1}$ ) using the singular value decomposition method (Lawson and Hanson[6]).

(b) Coda normalization method

Coda waves mainly consist of scattered S-wave. From the single-scattering model of Aki and Chouet[7], the spectral amplitude of coda waves ( $O_{ij}(f, t_c)$ ) can be expressed as

$$O_{ij}(f, t_c) = S_i(f)G_j(f)P(f, t_c) \quad (3)$$

where  $P(f, t_c)$  is the coda excitation factor that is independent of a locational relation of hypocenter and station for a lapse time ( $t_c$ ) greater than about twice the direct S-wave travel time. By dividing eq.(1) by eq. (3) and taking into consideration the hypothesis that  $S_i(f)$  and  $G_j(f)$  are common to S- and coda-wave, we obtain the following equation.

$$\ln \left( R_{ij} \frac{O_s(f)}{O_c(f, t_c)} \right) = \frac{-\pi f t_{ij}}{Q_s(f)} + \text{const.}(f) \quad (4)$$

where  $O_s$  and  $O_c$  are the spectra of the observed S- and coda-wave, respectively. Applying the least-squares method to plots of logarithm of coda-normalized amplitude (left-hand side of eq. (4)) against the S-wave travel time ( $t_{ij}$ ) for many earthquakes, we can estimate  $Q_s$  from the slope of a linear regression line.

**Data**

In this study, we tentatively divide the study area into three zones bounded by a coastline and the VF. Roughly speaking, these three zones correspond to a back-arc side mantle wedge (BAMW), a fore-arc side mantle wedge (FAMW) and a shallow descending plate or slab. The stations and the events used in the analyses for each study zone are as follows. In this study, the hypocenters, origin times and magnitudes of all events are taken from Japan Meteorological Agency (JMA).

Fig. 2(a) shows locations of the stations and events used in  $Q_s$  estimation of the FAMW. At these stations, three-components instruments have been installed, and we use two horizontal components (NS and EW) in the analyses. The stations used in the SI method are composed of the K-NET, F-net (NIED) and Central Research Institute of Electric Power Industry (CRIEPI). There are 17 stations in all. Two stations, NMR and AKS, are considered to be a rock site. NMR is the F-net station where strong motion velocity seismometer, VSE-355G2, is placed on a horizontal tunnel in the Cretaceous hard mud or sandstone. We

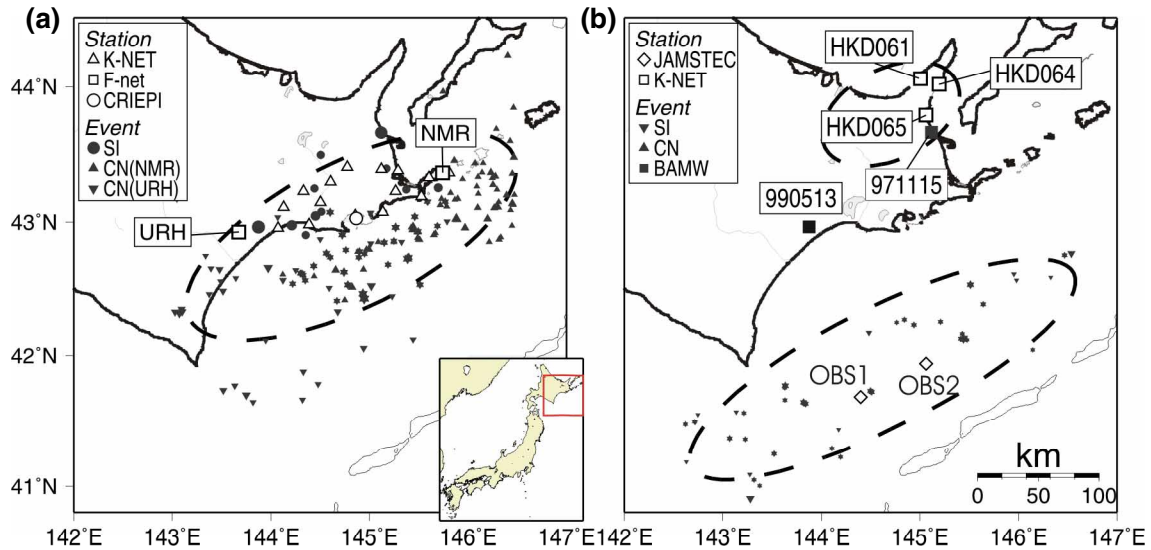


**Figure 2. Location map showing epicenters and stations used. Left: the map for FAMW, and right: that for BAMW and plate.**

use strong-motion data from 13 intermediate-depth events having magnitudes from 3.9 to 6.4, and depths from about 90 to 150km. In the CN method, two F-net stations, NMR and URH, are used. At URH, strong motion velocity seismometer, VSE-355G, is placed on a horizontal tunnel. Qs estimation is separately performed for each station, and 108 and 73 events are analyzed for NMR and URH, respectively. These events, occurring from May, 1997 to April, 2002, have magnitudes from 4.0 up to 6.4 and focal depths between 30 and 160km.

In the back-arc side region of the VF, data set is incomplete due to few records, thus we cannot apply above-mentioned two methods for the BAMW. Then we perform simple evaluation of Qs value for the BAMW as mentioned later.

We especially use data obtained by ocean bottom seismometers (OBS) for plate Qs estimation. The stations and events used are shown in Fig. 2(b) together with those for the BAMW. A real time seafloor cabled observation system has been installed in July, 1999 by Japan Marine Science and Technology Center (JAMSTEC) at the continental slope in the southern Kurile subduction zone approximately 100 to 150 km off the southern Hokkaido coast (Hirata et al.[8]). This system consists of three ocean bottom seismometer stations and each station has a three-components acceleration detector. Since gimbals units are not used in the OBS, the directions of the three axes of each OBS are rotated. We use one of two horizontal-component accelerometers that have a small dip angle (less than  $2.3^\circ$ ). In this study, we use the data obtained at two stations, OBS1 and OBS2, which are located approximately parallel to the Kurile trench axis. The events occurring from August, 2000 to June, 2002 are used. In the SI method, 83 records

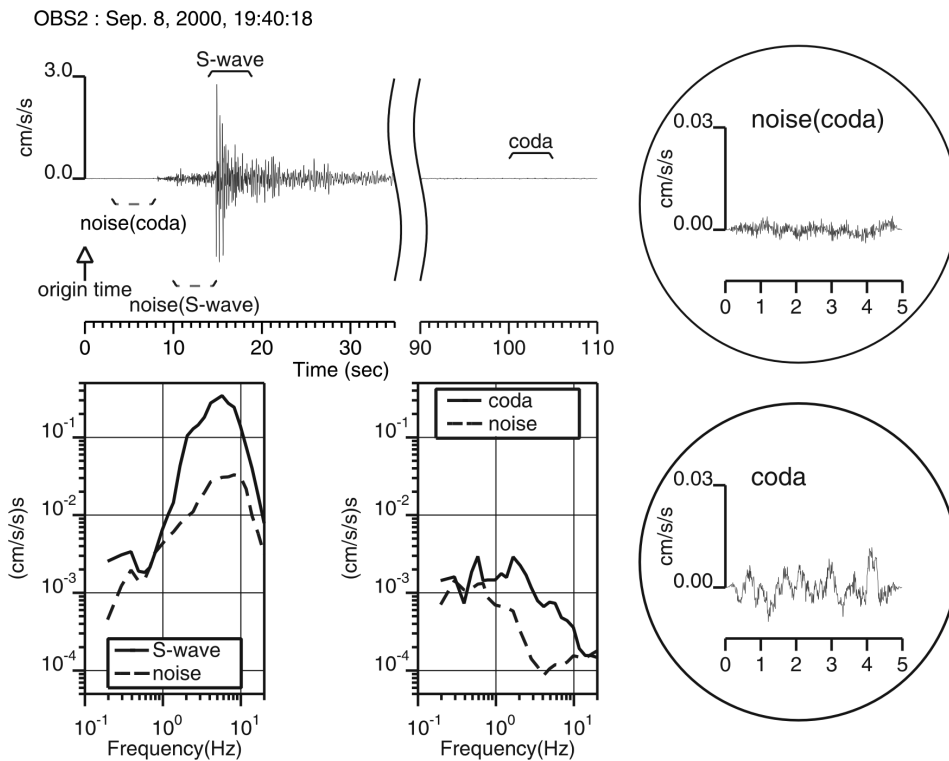


**Figure 3. (Top) A typical example of the horizontal-component accelerograms. Note the discontinuous time axis. Time windows for the spectral analysis are also shown; S-wave, coda, S noise and coda noise. (Bottom) Acceleration Fourier spectra of S-wave and its noise (left) and those of coda and its noise (right).**

from 50 events that have magnitudes from 3.0 up to 4.8 and focal depths between 30 and 70 km are analyzed. On the other hand, in the CN method, 60 records (OBS1: 30, OBS2: 30) from 37 events that have magnitudes from 3.0 to 4.5 and focal depths from 30 to 65km are analyzed.

Fig. 3 shows the observed acceleration time histories and Fourier amplitude spectra at OBS2 from the Sep. 8, 2000 event as an example. The time windows for the calculation of the Fourier spectra are set to 5-sec for plate zone analyses and 10-sec for other cases, and a cosine-shaped taper at 10% each end of the time window are applied. The coda window is defined as it starts at 100 sec after the event origin time for all events. Two portions of the seismograms, before the S-wave arrival and the P-wave arrival, are used in calculation of the noise spectra for S-wave and coda wave, respectively. Fourier amplitude spectra are calculated by Fast Fourier Transform (FFT). The logarithms of the amplitude spectra are then smoothed by averaging the amplitudes within the range of  $\pm f_c/5$  ( $f_c$ , center frequency). The 25 center frequencies are chosen as they distribute logarithmically at common interval from 0.1 to 20 Hz. Except the case of plate zone analyses, two horizontal components are summed vectorially in the SI method. In the CN method, however, we use each component separately. We use only data with a signal-to-noise ratio greater than 2 at each frequency.

## RESULTS

Fig. 4 summarizes the results.

### FAMW

The solid and open circles show the  $Q_s$  values estimated by the SI method and the CN method, respectively. The result of the CN method is the averaged one from NMR and URH results. These  $Q_s$  values increase with frequencies and then we fit a power law for the frequency dependence. We obtain  $Q_s=62.5f^{1.16}$  by the SI method and  $Q_s=74.3f^{0.97}$  by the CN method for frequency range from 1 to 10Hz.  $Q_s$  values from two methods are very similar as shown in Fig. 4.

### BAMW

As mentioned above, we cannot apply two methods of  $Q_s$  estimation to the data set for this zone because of few records. Then we try another method. A simplified  $Q_s$  structure that consists of two zones bounded by the VF is assumed. Since we have already estimated the source spectra and  $Q_s$  value by SI method for the FAMW,  $Q_s$  value for the BAMW can be roughly estimated by observed spectral ratios from those events at stations located on back-arc side of the VF. The spectral ratio is expressed as follows,

$$\frac{O_1}{O_2} = \frac{R_1^{-1} S_1 \exp(-\pi f R_1 / Q_1 V_s)}{R_2^{-1} S_2 \exp(-\pi f R_2 / Q_2 V_s)}$$

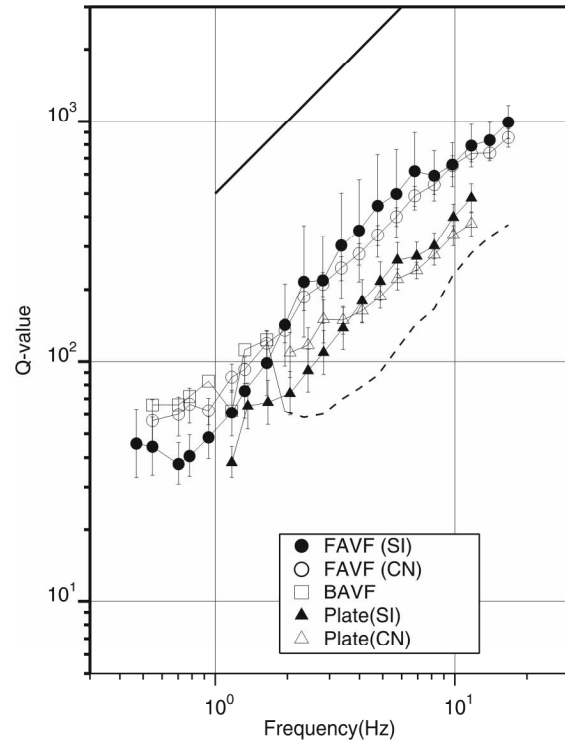


**Figure 4.  $Q_s$  values in the subduction zone. Solid and open circles are the  $Q_s$  value for the FAMW by spectral inversion method and coda normalization method, respectively. Solid and open triangles are those for the plate by spectral inversion and coda normalization method, respectively. Open squares are those for the BAMW. The error bars indicate the standard deviation. Bold line represent  $Q_s=500f$ .**

$R_1$  and  $R_2$  can be divided into two segments corresponding to two zones bounded by the VF, and then  $Q_1$  and  $Q_2$  are also divided into those value in two zones ( $R/Q=R_{fore}/Q_{fore} + R_{back}/Q_{back}$ ). For the estimation, three K-NET stations (HKD061, HKD064 and HKD065) and two intermediate-depth events (971115 and 990513) shown in Fig.2 (b) are used and  $V_s=4.3\text{km/sec}$  is assumed. Events 971115 and 990513 have focal depth of about 150km and 100km, respectively. Since the observed spectra from event 971115 have low S/N ratios at frequencies higher than about 2 Hz, it is impossible to estimate  $Q_s$  values quantitatively. Those  $Q_s$  values, however, are considered to be an upper limit.  $Q_s$  values estimated by the spectral ratio for three stations are similar one another and those from HKD061 are shown in Fig. 4 as representative. The big difference of  $Q_s$  value between the FAMW and BAMW is the strength of frequency dependence.

### Plate

In this study zone, the assumption of a homogeneous structure is not suitable, because of shallow focal depths compared with epicentral distances. Then we assume the 1-D stratified structure for analysis. In the layered structure,  $R_{ij}$  of eq. (2) is expressed as  $R_{ij} = \mathfrak{R}_{ij}^{-1} \sqrt{\rho_g \beta_g / \rho_s \beta_s} \prod_l T_l$ , where  $\mathfrak{R}_{ij}^{-1}$  represents geometrical spreading,  $T_l$  is the transmission coefficient at the  $l$ -th interface.  $\rho_s$  and  $\beta_s$  are the density and the S-wave velocity at the source, and  $\rho_g$  and  $\beta_g$  are those at the site, respectively. In this study,  $\mathfrak{R}_{ij}^{-1}$  and  $T_l$  are calculated by dynamic ray tracing (Červený et al.[9]) assuming the 1-D velocity structure under the stations (Fig. 5). This structure is constructed based on the 2-D P-wave velocity structure in the southern Kurile trench deduced from ocean bottom seismographic refraction studies (Iwasaki et al.[10]).  $\rho$  and  $\beta$  are taken from this 2-D structure ( $\beta = \alpha / \sqrt{3}$ ,  $\rho = 1.7 + 0.2\sqrt{3}\beta$ ). In Fig. 4, solid and open triangles show the  $Q_s$  values estimated by the SI method and the CN method, respectively. These  $Q_s$  values increase with frequencies like those for the FAMW, and then we fit a power law for the frequency dependence. We obtain  $Q_s=38.6f^{1.03}$  by the SI method and  $Q_s=65.6f^{0.69}$  by CN method. The CN results are the averaged one for two stations calculated by the same manner as the FAMW. Fig.5 shows a diagram of seismic rays from the events used to the station OBS2, and we know that the majority of the ray passes through the upper mantle in the plate and the ray length passing through the crust is nearly the same for all events. That's why, these  $Q_s$  values are considered to be an averaged value in the upper part of the plate. The  $Q_s$  values from two methods are very similar, and those for two zones, the FAMW and plate, are nearly the same.

### $Q_s$ MODEL OF PLATE

At the island-arc regions, abnormal distributions of seismic intensity are observed during the inter-plate

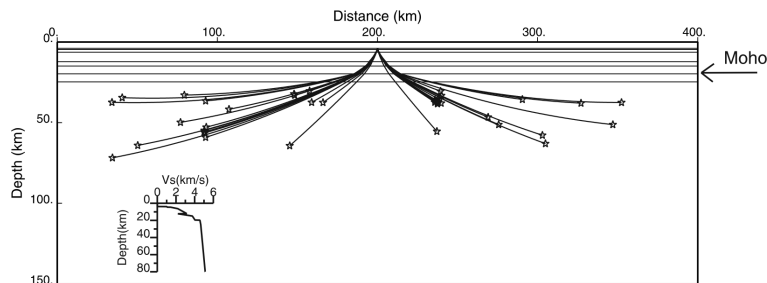


**Figure 5. Diagram of seismic rays from the events (open stars) to the station OBS2. The OBS2 is located at the center (200km point). The velocity profile assumed is also shown in the lower half of the figure.**

and intra-slab earthquakes. This phenomenon is explained by the existence of anomalous upper mantle structure: seismic waves can propagate more effectively in the high-Q slab than surrounding low-Q mantle. Fig. 4 shows that  $Q_s$  values in the plate and FAMW do not have large difference, and it seems to be contrary to the past research results. In generally, seismic waves propagating from the far hypocenter pass through deeper parts of the plate, while seismic rays used in this study mainly pass through the upper part of the Pacific plate which has a thickness of about 100km around studied area (Fig. 5). Thus, in this section, we hypothesize the two-layered  $Q_s$  structure in the plate and estimate the depth of the boundary and the  $Q_s$  value for the deeper layer.

Fig. 6(a) shows locations of the earthquakes and stations used. All stations are deployed by NIED. NMR is the F-net station as mentioned before. S-wave velocity  $V_s$  is unknown but we surmise that  $V_s$  is 1.7km/sec from the velocity structure of near borehole station. AOMH17 and IWTH23 are the KiK-net stations, located on north-eastern Japan, where the strong motion accelerometers have been equipped on the ground surface and in the borehole. The velocity structures down to about 100m have been investigated by NIED at KiK-net stations, and we can estimate the incident wave at bottom of the borehole. Since  $V_s$  at bottom of AOMH17 and IWTH23 is 1.45km/sec and 2.20km/sec, respectively, we can consider that the records at three stations are observed at a basement having almost the same  $V_s$ , after correcting the effects of surface layers. Fig. 6(b) shows an assumed  $Q_s$  structure. The circle and the triangles indicate a hypocenter and stations, respectively. The right-hand side region of the circle corresponds to the FAMW of eastern Hokkaido and  $Q_1=62.5f^{1.16}$  is assumed. On the other hand, the left-hand side region of the circle corresponds to the Pacific slab or plate and  $Q_2=38.6f^{1.03}$  is assumed for the upper layer. In this model, there are two unknown parameters, the depth of the boundary ( $H$ ) and the  $Q_s$  values in the lower layer ( $Q_3$ ), and they are estimated by following procedure.

- 1) The source spectrum is estimated from the observed spectrum at NMR by correcting the site and the path effects. The observed S-wave spectrum was calculated by FFT and the time window is set to 10-sec with a cosine-shaped taper (at 10% each end of the time window). The site amplification factor at NMR is assumed to be 2 for all frequencies and the geometrical spreading is calculated by the ray tracing for 1-D velocity structure that explains the observed S-wave travel time at Hokkaido-Tohoku regions.
- 2) The synthetic spectra at AOMH17 and IWTH23 are calculated using the estimated source spectrum and the assumed two-layer  $Q_s$  structure. Here, we assume  $H$  at intervals of 10km from 30km to 80km and  $Q_3$  of 100f, 200f, 500f and 1000f.
- 3) The observed spectra at basement of two KiK-net stations are calculated by correcting the site effects. The observed S-wave spectra are calculated by the same manner as NMR. The site effects are evaluated by the Propagator Matrix method (Aki and Richards[11]) for the case of vertical incident of SH wave.
- 4) The synthetic and observed spectra for 2 stations from 3 events are compared and then  $H$  and  $Q_3$  are estimated from the good agreement case.

In Fig. 7, the case of  $H= 40, 50, 60$ km and  $Q_3 = 100f, 500f$  are shown as an example. This figure shows that the case of  $H=50$ km and  $Q_3=500f$  suits best. In this study zone, the thickness of the Pacific plate is considered to be about 100km and the earthquakes are occurring within the top 50km in the plate. Although we do not have an exact idea, there may be some correlation between the thickness of the seismic zone and that of upper layer of attenuation model in this study. This study zone corresponds to the portion at which Pacific plate begins to subduct. In the region before the Pacific plate begins to sink,  $Q_s=180f$  (Butler et al.,[12]) and  $Q_s=500f$  (Kubo et al.[13]) have been estimated at almost the same frequency range as this study, and their  $Q_s$  values are very similar with our lower plate's  $Q_s$  value. In the portion of plate bending, it is considered that the upper part becomes a tension field and the lower part becomes compressing field. The two-layer  $Q_s$  structure might reflect such stress condition.

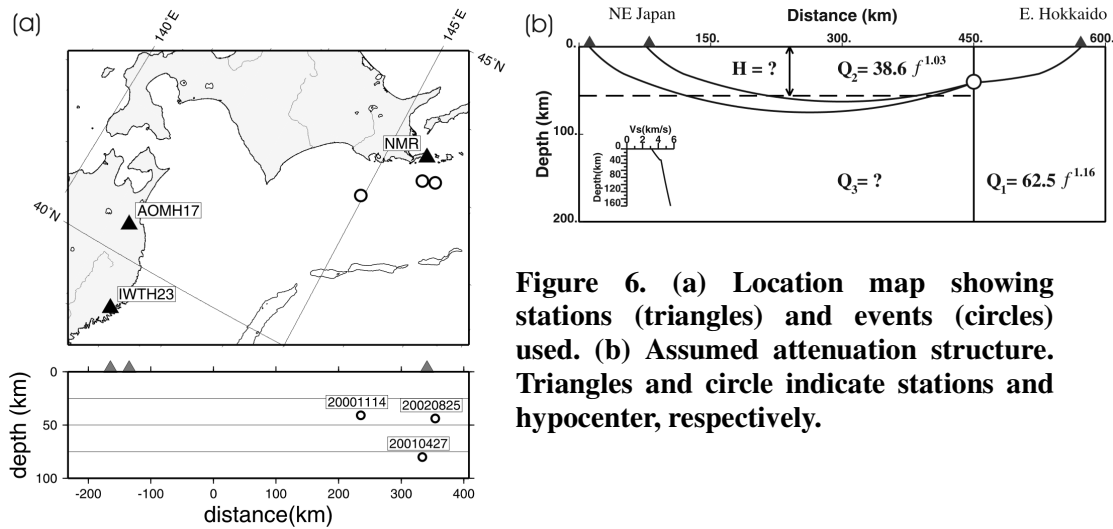


**Figure 6. (a) Location map showing stations (triangles) and events (circles) used. (b) Assumed attenuation structure. Triangles and circle indicate stations and hypocenter, respectively.**

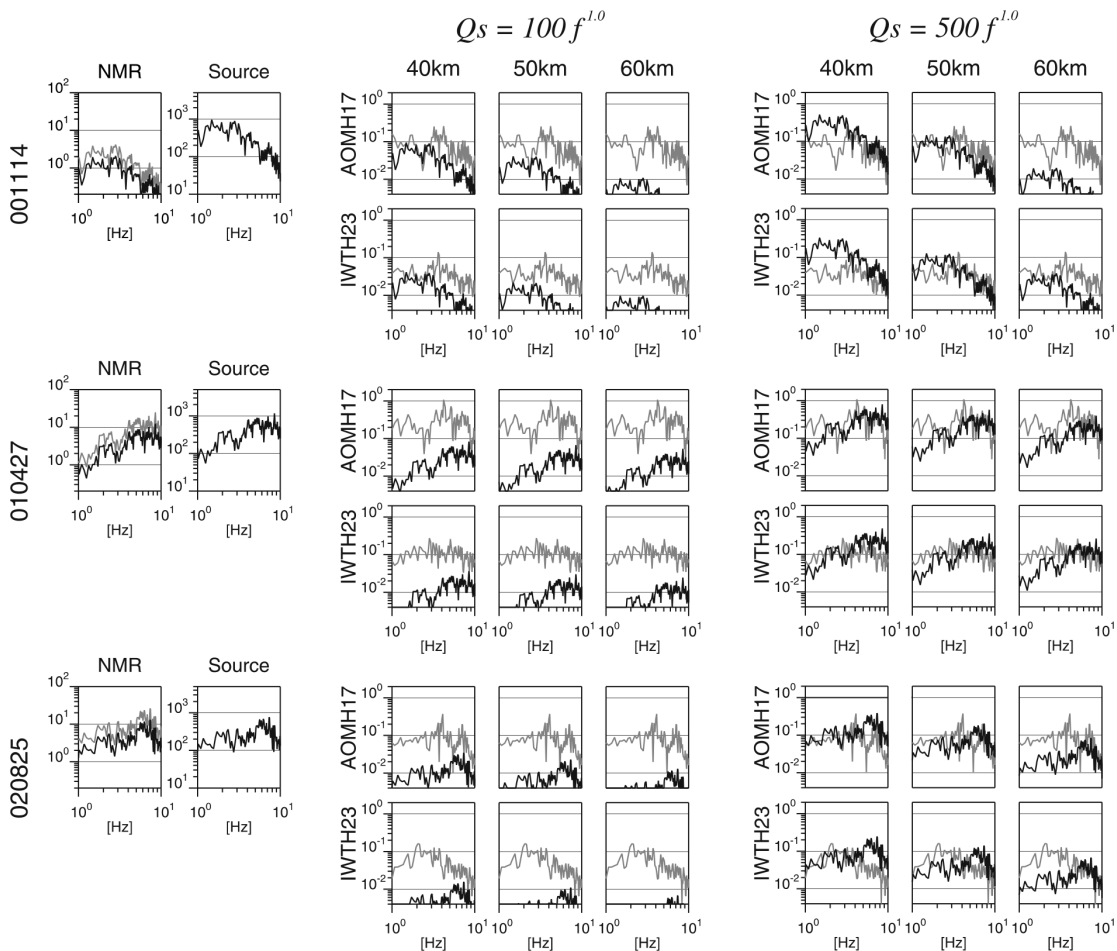


**Figure 7. Comparison of observed (black) and synthetic (gray) spectra.**

## CONCLUSION

We estimated the S-wave attenuation factor ( $Q_s$  value) in the southernmost Kurile-Hokkaido subduction zone. Two techniques of  $Q_s$  estimation, the spectral inversion method (SI) and the coda-normalization method (CN) were used. In the FAMW, we obtained  $Q_s=62.5f^{1.16}$  by the SI method and  $Q_s=74.3f^{0.97}$  by the CN method for frequency range from 1 to 10Hz. In the plate  $Q_s$  estimation, we used the data from OBS stations because the seismic rays pass mainly through the plate and calculate geometrical spreading by dynamic ray tracing. We obtained  $Q_s=38.6f^{1.03}$  by the SI method and  $Q_s=65.6f^{0.69}$  by CN method. The  $Q_s$ -values for these two zones were nearly the same and show strong frequency-dependence. The  $Q_s$ -values obtained from two methods were nearly the same. While in the BAMW, we could not apply above two methods due to few records. We evaluated  $Q_s$  values for the BAMW by some assumptions, however, and we concluded that the  $Q_s$ -values for the BAMW had considerably weak frequency-dependence compared with the other two zones. Finally we estimated  $Q_s$  value for deeper part of the plate and obtained that  $Q_s=500f$  for the plate deeper than 50km. We concluded that the anomalous upper mantle attenuation structure beneath the eastern Hokkaido reflected the difference in the frequency-dependence of  $Q_s$ -value at high-frequencies (>1Hz). The laterally heterogeneous  $Q_s$  structure obtained in this study is useful for predicting strong ground motion from large inter-plate and intra-slab earthquakes.

## ACKNOWLEDGEMENTS

The authors are grateful to Dr. M. Horike for providing his computer code for the ray tracing. Strong motion data are provided by NIED (K-NET, F-net and KiK-net) and CRIEPI. The OBS data used in this study are provided by JAMSTEC.

## REFERENCES

1. Umino N., Hasegawa A. "Three-dimensional  $Q_s$  structure in the northeastern Japan arc (in Japanese)", *Zisin II*, 1984, 37, 217-228.
2. Nakamura R., Uetake T. "Three dimensional attenuation structure and site amplification inversion by using a large quantity of seismic strong motion records in Japan", paper presented at 12th World Conference on Earthquake Engineering, Auckland, New Zealand, Jan. 30 to Feb. 4, 2000, ID 0724.
3. Tsumura N., Matsumoto S., Horiuchi S., and Hasegawa A. "Three-dimensional attenuation structure beneath the northeastern Japan arc estimated from spectra of small earthquakes", *Tectonophysics*, 2000, 319, 241-260.
4. Iwata T., Irikura K. "Source parameters of the 1983 Japan Sea earthquake sequence", *J. Phys. Earth*, 1988, 36, 155-184.
5. Aki K. "Attenuation of shear-waves in the lithosphere for frequencies from 0.05 to 25 Hz", *Phys. Earth Planet. Inter.*, 1980, 21, 50-60.
6. Lawson C. L., Hanson R. J. "Solving Least Squares Problems". Prentice-Hall, Inc., Englewood Cliffs, New Jersey, 1974.
7. Aki K., Chouet B. "Origin of coda waves: source, attenuation and scattering effects", *J. Geophys. Res.*, 1975, 80, 3322-3342.
8. Hirata K., Aoyagi M., Mikada H., Kawaguchi K., Member IEEE, Kaiho Y., Iwase R., Morita S., Fujisawa I., Sugioka H., Mitsuzawa K., Suyehiro K., Kinoshita H., Fujiwara N. "Real-time geophysical measurements on the deep seafloor using submarine cable in the southern Kurile subduction zone". *IEEE J. Ocean. Eng.*, 2002, 27, No. 2, 170-181.
9. Iwasaki T., Shiobara H., Nishizawa A., Kanazawa T., Suyehiro K., Hirata N., Urabe T., Shimamura H. "A detailed subduction structure in the Kuril trench deduced from ocean bottom seismographic refraction studies", *Tectonophysics*, 1989, 165, 315-336.

10. Červený V., Molotkov I. A., Psenvik I. "Ray method in seismology", Univerzita Karlova, Praha, 1977.
11. Aki K., Richards P. G. "Quantitative Seismology, Vol. 1." W. H. Freeman & Co., San Francisco, California. 1980.
12. Butler R., McCreery C. S., Frazer L. N., Walker D. A. "High-frequency seismic attenuation of oceanic P and S waves in the Westerns Pacific". J. Geophys. Res., 1987, 92, 1383-1396.
13. Kubo A., Ouchi T., Shimamura H. "Envelope broadening and spatial attenuation of S-waves in the oceanic lithosphere". Mem. Grad. School Sci. and Technol., Kobe Univ., 1995, 13-A, 101-116.